

1 **IDENTIFICATION OF DYNAMIC MICROBIAL SIGNATURES IN**  
2 **LONGITUDINAL STUDIES**

3 Short running title: Microbiome signatures in longitudinal studies

4 M.Luz Calle<sup>1\*</sup>, Antoni Susin<sup>2</sup>

5 <sup>1</sup> Biosciences Department, Faculty of Sciences and Technology, University of Vic -  
6 Central University of Catalonia, Vic, Spain

7 <sup>2</sup> Mathematical Department, UPC-Barcelona Tech, Barcelona, Spain

8 \*Corresponding author: M.Luz Calle, Biosciences Department, Faculty of Sciences and  
9 Technology, University of Vic - Central University of Catalonia, Carrer de la Laura, 13,  
10 08500-Vic, Spain

11 Tel: +34938861222 Email: malu.calle@uvic.cat

12

13 **Abstract**

14 The study of microbiome dynamics is key for unveiling the role of the microbiome in  
15 human health. Addressing the compositional structure of microbiome data is  
16 particularly critical in longitudinal studies where compositions measured at different  
17 times can yield to different subcompositions.

18 We propose a new compositional data analysis (CoDA) algorithm for inferring dynamic  
19 microbial signatures. The algorithm performs penalized regression over the summary of  
20 the log-ratio trajectories (the area under these trajectories) and the inferred microbial  
21 signature is expressed as a log-contrast model. Graphical representations of the results  
22 are provided to facilitate the interpretation of the analysis: plot of the log-ratio  
23 trajectories, plot of the signature and plot of the prediction accuracy of the model. The  
24 new proposal is illustrated with data on the developing microbiome of infants.

25 The algorithm is implemented in the R package “code4microbiome” ([https://cran.r-](https://cran.r-project.org/web/packages/coda4microbiome/)  
26 [project.org/web/packages/coda4microbiome/](https://cran.r-project.org/web/packages/coda4microbiome/)) that is accompanied with a vignette with  
27 a detailed description of the functions. The website of the project contains several  
28 tutorials: <https://malucalle.github.io/coda4microbiome/>

29

30 **Key-words:** log-ratio analysis, longitudinal studies, microbiome analysis, microbiome  
31 signatures, penalized regression

32

33

34

35

## 36 **1. Introduction**

37 Microbiome composition is dynamic and the study of microbiome changes over time is  
38 of primary importance for understanding the relationship between microbiome and  
39 human phenotypes. Longitudinal studies are costly, both economically and logistically,  
40 but there is growing evidence of the limitations of cross-sectional studies for providing  
41 a full picture of the role of the microbiome in human health. Microbiome longitudinal  
42 studies can be very valuable in this context, provided appropriate methods of analysis  
43 are used (Schmidt et al. 2018)

44 Microbiome data analysis is challenging because, among other things, the  
45 compositional nature of the data (Susin et al. 2020, Calle 2019, Gloor et al. 2016, 2017,  
46 Gloor and Reid, 2016). This is particularly critical in the context of microbiome  
47 longitudinal studies where compositions measured at different times can be affected by  
48 distinct batch effects and similar quality control or filtering protocols may yield to  
49 different subcompositions at each time point.

50 The log-ratio approach (Aitchison 1986), that consists in analyzing the abundances of  
51 some taxa relative to the abundances of other taxa, is subcompositionally coherent and  
52 provides an especially interesting standpoint for exploring microbiome dynamics. In  
53 longitudinal studies, the log-ratio between two groups of taxa measured at different time  
54 points gives a curve profile or trajectory for each sample. We propose to explore the  
55 association between the phenotype of interest and the shape of the log-ratio microbiome  
56 trajectories.

57 Among the questions outstanding about microbiome dynamics, we focus on inferring  
58 dynamic microbial signatures and propose a novel algorithm to identify a set of  
59 microbial taxa whose joint dynamics is associated with the phenotype of interest. For

60 binary outcomes, such as disease status, we aim to identify two groups of taxa with  
61 clearly different log-ratio trajectories for cases and controls.

62 The algorithm performs variable selection through penalized regression over the  
63 summary of the log-ratio trajectories (the area under these trajectories). The inferred  
64 microbial signature is expressed as a log-contrast model (Aitchison, J. and Bacon-  
65 Shone, J. 1984), i.e. a log-linear model with the constraint that the sum of the  
66 coefficients is equal to zero. The zero-sum constraint ensures the invariance principle  
67 required for compositional data analysis.

68 The interpretability of results is of major importance in the context of microbiome  
69 studies. We provide several graphical representations of the results that facilitate the  
70 interpretation of the analysis: plot of the log-ratio trajectories, plot of the signature  
71 (selected taxa and coefficients) and plot of the prediction accuracy of the model.

72 The methodology is illustrated with data from the “Early childhood and the microbiome  
73 (ECAM) study” (Bokulich et al. 2016).

74 The algorithm is implemented in the R package “code4microbiome” ([https://cran.r-  
75 project.org/web/packages/coda4microbiome/](https://cran.r-project.org/web/packages/coda4microbiome/)) that is accompanied with a vignette with  
76 a detailed description of the functions. The website of the project contains several  
77 tutorials: <https://malucalle.github.io/coda4microbiome/>

78

79

## 80 2. Materials and methods

81 We first describe the analysis of log-ratios between two taxa A and B in longitudinal  
82 studies, which involves the summary of the log-ratio trajectories. Then we explain how  
83 to generalize the analysis of pairwise log-ratios to identify microbial signatures  
84 involving more than two taxa.

### 85 Log-ratio analysis and taxa prioritization

86 Assume  $n$  subjects with fixed phenotype  $Y = (Y_1, \dots, Y_n)$ . Subject  $i$  has been observed in  
87  $L_i$  time points,  $(t_{i1}, t_{i2}, \dots, t_{iL_i})$ . We denote by  $X_i(t_{ij}) = (X_{i1}(t_{ij}), X_{i2}(t_{ij}), \dots, X_{iK}(t_{ij}))$   
88 the microbiome composition of subject  $i$  at time  $t_{ij}$ , where  $K$  is the number of taxa  
89 which is assumed to be the same for all the individuals and all the time points.  $X_i(t_{ij})$   
90 can represent either relative abundances (proportions) or raw counts. We denote by  
91  $\log X_i(t_{ij})$  the logarithm transformation of microbiome abundances after zero  
92 imputation. The log-abundance trajectory of component A for individual  $i$  is denoted by  
93  $\log X_{iA} = (\log X_{iA}(t_{i1}), \log X_{iA}(t_{i2}), \dots, \log X_{iA}(t_{iL_i}))$  and the log-ratio trajectory  
94 between components A and B for individual  $i$  is given by:

$$\begin{aligned} 95 \quad \log X_{iA} - \log X_{iB} &= (\log X_{iA}(t_{i1}) - \log X_{iB}(t_{i1}), \\ 96 \quad &\log X_{iA}(t_{i2}) - \log X_{iB}(t_{i2}), \dots, \log X_{iA}(t_{iL_i}) - \log X_{iB}(t_{iL_i})) \end{aligned}$$

97 We summarize the log-ratio trajectories within two time points  $l_1$  and  $l_2$  as the integral  
98 of the log-ratio trajectory:

$$99 \quad s_i(A, B) = \int_{l_1}^{l_2} (\log X_{iA}(t) - \log X_{iB}(t)) dt \quad (1)$$

100 where the values of the log-ratio for  $t \notin (t_{i1}, t_{i2}, \dots, t_{iL_i})$  are linearly interpolated.

101 We do not take the absolute value in equation (1) because the sign of the integral is  
102 informative: Positive values of  $s_i(A, B)$  correspond to trajectories of component A  
103 above trajectories of component B, that is, larger relative abundances of A with respect  
104 to B, while negative values represent the opposite. Values of  $s_i(A, B)$  around zero can  
105 represent similar abundances between A and B over time or a non-homogeneous trend  
106 between A and B within the observed region.

107 Another advantage of the summary  $s_i(A, B)$  is computational. Since the integral is  
108 linear,  $s_i(A, B)$  is equal to the difference between the integrals of log-transformed  
109 microbiome abundances of taxa A and taxa B:

$$110 \quad s_i(A, B) = \int_{l_1}^{l_2} \log X_{iA}(t) dt - \int_{l_1}^{l_2} \log X_{iB}(t) dt$$

111 Thus, the number of integrals to be calculated is of the order of  $K$ , the number of taxa,  
112 instead of  $K(K - 1)/2$ , the number of pairwise log-ratios.

113 The log-ratio summary for the  $n$  subjects,  $s(A, B) = (s_1(A, B), \dots, s_n(A, B))$ , can be  
114 tested for association with the phenotype  $Y = (Y_1, \dots, Y_n)$  with a generalized linear  
115 model (glm) adjusted for some covariates  $Z$ :

$$116 \quad g(E(Y_i)) = \beta_0 + \beta_1 \cdot s_i(A, B) + \gamma' \cdot Z_i \quad (2)$$

117 where  $\beta_0$  is the intercept,  $\beta_1$  is the regression coefficient for the log-ratio summary  
118 between components A and B,  $Z = (Z_1, Z_2, \dots, Z_r)$  are non-compositional covariates and  
119  $\gamma$  is the vector of regression coefficients for  $Z$ .

## 120 **Microbiome signature based on log-ratio analysis**

121 To identify those log-ratios that are most associated with the outcome  $Y$ , we implement  
122 glm penalized regression on the log-ratio summaries for all pairs of taxa:

123 
$$g(E(Y)) = \beta_0 + \sum_{j \in J} \beta_j \cdot S(j) \quad (3)$$

124 where  $J = \{1, \dots, K(K-1)/2\}$  and  $S(j) = s(j_1, j_2)$  is the log-ratio summary of  
125 components  $j_1$  and  $j_2$  with  $(j_1, j_2) \in J_{12}$ , the set of all possible combinations of pairs of  
126 components.

127 The regression coefficients in equation (3) are estimated to minimize a loss function  
128  $L(\beta)$  subject to a penalization on the regression coefficients,  $P(\beta)$ :

129 
$$\hat{\beta} = \underset{\beta}{\operatorname{argmin}}\{L(\beta) + P(\beta)\} \quad (4)$$

130 For the penalty term we consider the elastic-net, which combines the L1 and L2 norms:  
131  $P(\beta) = \lambda_1 \|\beta\|_2^2 + \lambda_2 \|\beta\|_1$ . A common reparameterization of  $P(\beta)$  is  $\lambda_1 = \lambda(1 - \alpha)/2$   
132 and  $\lambda_2 = \lambda\alpha$  where  $\lambda$  controls the amount of penalization and  $\alpha$  the mixing between the  
133 two norms.

134 For the linear regression model the loss function is given by the residual sum of squares

135 
$$\hat{\beta} = \underset{\beta}{\operatorname{argmin}}\{\|Y - S\beta\|_2^2 + \lambda_1 \|\beta\|_2^2 + \lambda_2 \|\beta\|_1\},$$

136 where  $S$  is the matrix of all log-ratio summaries and has dimension  $n$  by  $K(K-1)/2$ .

137 The expression of the optimization problem (4) for other models, like the logistic  
138 regression and the multinomial regression models, can be found in Friedman et al.

139 (2010). Non-compositional covariates  $Z$  are previously modeled with  $Y$  and the fitted  
140 values are considered as “offset” in the penalized regression.

141 The result of the penalized optimization provides a set of selected pairs of taxa, those  
142 with a non-null estimated coefficient. For each individual,  $i \in \{1, \dots, n\}$ , the linear  
143 predictor of the generalized linear model (3),  $M_i = \sum_{j \in J, (j_1, j_2) \in J_{12}(j)} \hat{\beta}_j \cdot s_i(j_1, j_2)$ , is the  
144 microbiome signature which is associated with the phenotype  $Y_i$ . Because of the  
145 linearity of the integrals used as summaries of the log-ratio trajectories, the microbiome  
146 signature  $M$  can be rewritten in terms of the selected single taxa which is more  
147 interpretable than the selected pairs of components:

$$\begin{aligned}
 148 \quad M &= \sum_{j \in J, (j_1, j_2) = J_{12}(j)} \hat{\beta}_j \cdot s(j_1, j_2) = \\
 149 \quad &= \sum_{j \in J, (j_1, j_2) = J_{12}(j)} \hat{\beta}_j \cdot \int_{l_1}^{l_2} \log X_{j_1}(t) dt - \sum_{j \in J, (j_1, j_2) = J_{12}(j)} \hat{\beta}_j \cdot \int_{l_1}^{l_2} \log X_{j_2}(t) dt = \\
 150 \quad &= \sum_{k=0}^K \hat{\theta}_k \cdot \int_{l_1}^{l_2} \log X_k(t) dt = \\
 151 \quad &= \int_{l_1}^{l_2} (\sum_{k=0}^K \hat{\theta}_k \cdot \log X_k(t)) dt \\
 152 \quad & \tag{5}
 \end{aligned}$$

153 where  $\hat{\theta}_k = \sum_{j:k \in J_{12}(j)} \hat{\beta}_j$ , that is, the sum of the coefficients  $\hat{\beta}_j$  corresponding to a log-  
 154 ratio that involves component  $k$ .

155 It can be proved that  $\sum_{k=0}^K \hat{\theta}_k = 0$  and thus, the microbiome signature  $M$  is the integral  
 156 of the trajectory of a log-contrast function involving the selected taxa (those with  $\hat{\theta}_k \neq$   
 157 0). This ensures the invariance principle required for proper compositional data analysis  
 158 and it facilitates the interpretation of the microbiome signature: Expression  $\sum_{k=0}^K \hat{\theta}_k \cdot$   
 159  $\log X_k(t)$  in (5) can be interpreted as a weighted balance between two groups of taxa,  
 160  $G_1$  and  $G_2$ , the taxa with a positive coefficient vs those with a negative coefficient  
 161 (Susin et al. 2020).

162 The package “coda4microbiome” (Calle and Susin, 2022) contains several functions  
 163 that implement the proposed algorithms. The two main functions are  
 164 `explore_lr_longitudinal()`, that implements the simple generalized linear model  
 165 (equation 2), and `coda_glmnet_longitudinal()`, that performs penalized regression for  
 166 the multivariable generalized linear model (equation 4). Additional functions are  
 167 available like function `plot_signature_curves()` that provides a plot of the signature



168 trajectories or `filter_longitudinal()` that filters those individuals and taxa with  
169 enough longitudinal information.

170 To illustrate the proposed approach and the R implementation we use data from the  
171 early childhood and the microbiome (ECAM) study (Bokulich et al. 2016). Metadata  
172 and microbiome data were downloaded from [https://github.com/caporaso-](https://github.com/caporaso-lab/longitudinal-notebooks)  
173 [lab/longitudinal-notebooks](https://github.com/caporaso-lab/longitudinal-notebooks). Microbiome data, corresponding to 16S rRNA gene  
174 microbiota compositions sampled at regular intervals, were available in QIIME 2 qza  
175 file format (file `ecam-table-genus.qza`) and were transformed to R objects with function  
176 `read_qza()` of the R library `qiime2R`: <https://github.com/jbisanz/qiime2R>. Metadata  
177 (file `ecam-sample-metadata.tsv`) were in long format: multiple rows for individual, one  
178 for each time-point observation. Initially the data contained information on 43 child and  
179 445 taxa at the genus level. We filtered those individuals and taxa with enough  
180 information for time-course profiling: we removed individuals with only one time-point  
181 observation and those taxa with less than 30 children (70% of individuals) with at least  
182 3 non-zero observations over the follow-up period. After filtering, the data reduced to  
183 42 children and 37 taxa.

### 184 **3. Results**

185 We demonstrate the proposed methodology with data from the “Early childhood and the  
186 microbiome (ECAM) study” that followed a cohort of 43 U.S. infants during the first 2  
187 years of life for the study of their microbial development and its association with early-  
188 life antibiotic exposures, cesarean section, and formula feeding (Bokulich et al. 2016).  
189 Microbiome data were available for 43 child and 445 taxa at the genus level (Bokulich  
190 et al. 2018). After filtering those individuals and taxa with enough information for time-  
191 course profiling, the data were reduced to 42 child and 37 taxa. We focus on the effects

192 of the diet on the early modulation of the microbiome by comparing microbiome  
 193 profiles between children with breastmilk diet (bd) vs. formula milk diet (fd) in their  
 194 first 3 months of life.

195 **Most important taxa**

196 By implementing the pairwise log-ratio approach for longitudinal data (function  
 197 `explore_lr_longitudinal()`), we identified which taxa have more different dynamics  
 198 between bd and fd children in the first three months of life. Table 1 provides the top 15  
 199 taxa with more discriminative dynamics between both diets.

200 Table 1. Taxa with most different abundances between the two diets groups during the first  
 201 three months of life.  
 202

<b>Taxonomic assignment</b>	<b>More abundant group</b>
<i>"p_Proteobacteria;c_Gammaproteobacteria;o_Pasteurellales;f_Pasteurellaceae;g_Haemophilus"</i>	<b>bd</b>
<i>"p_Firmicutes;c_Bacilli;o_Bacillales;f_Staphylococcaceae;g_Staphylococcus"</i>	<b>bd</b>
<i>"p_Firmicutes;c_Clostridia;o_Clostridiales;f_Veillonellaceae;g_Veillonella"</i>	<b>fd</b>
<i>"p_Firmicutes;c_Clostridia;o_Clostridiales;f_Lachnospiraceae;g_Blautia"</i>	<b>fd</b>
<i>"p_Firmicutes;c_Clostridia;o_Clostridiales;f_Ruminococcaceae;g_1"</i>	<b>fd</b>
<i>"p_Firmicutes;c_Clostridia;o_Clostridiales"</i>	<b>fd</b>
<i>"p_Firmicutes;c_Clostridia;o_Clostridiales;f_Clostridiaceae"</i>	<b>fd</b>
<i>"p_Actinobacteria;c_Actinobacteria;o_Bifidobacteriales;f_Bifidobacteriaceae;g_Bifidobacterium"</i>	<b>bd</b>
<i>"p_Firmicutes;c_Clostridia;o_Clostridiales;f_Lachnospiraceae"</i>	<b>fd</b>
<i>"p_Bacteroidetes;c_Bacteroidia;o_Bacteroidales;f_Bacteroidaceae;g_Bacteroides"</i>	<b>bd</b>
<i>"p_Firmicutes;c_Bacilli;o_Lactobacillales;f_Lactobacillaceae;g_Lactobacillus"</i>	<b>bd</b>
<i>"p_Firmicutes;c_Erysipelotrichi;o_Erysipelotrichales;f_Erysipelotrichaceae;g_[Eubacterium]"</i>	<b>fd</b>
<i>"p_Firmicutes;c_Clostridia;o_Clostridiales;f_Lachnospiraceae;g_Coprococcus"</i>	<b>fd</b>
<i>"p_Firmicutes;c_Clostridia;o_Clostridiales;f_Lachnospiraceae;g_Dorea"</i>	<b>fd</b>
<i>"p_Firmicutes;c_Bacilli;o_Lactobacillales;f_Enterococcaceae;g_Enterococcus"</i>	<b>fd</b>

203

204

## 205 Microbiome signature

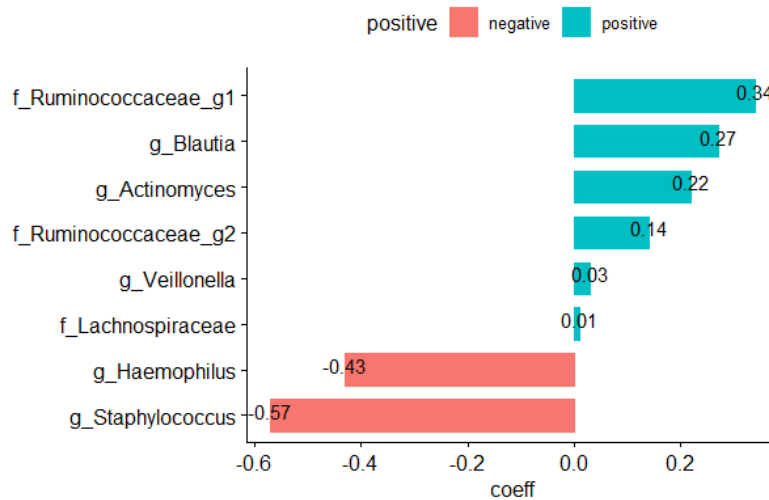
206 The application of the proposed algorithm (with function `coda_glmnet_longitudinal()`)  
 207 identified a microbiome signature with maximum discrimination accuracy between the  
 208 two diet groups. The signature is defined by the relative abundances of two groups of  
 209 taxa,  $G_1$  and  $G_2$ , where  $G_1$  is composed of 6 taxa (those with a positive coefficient in the  
 210 regression model) and  $G_2$  is composed of 2 taxa (those with a negative coefficient)  
 211 (Table 1 and Figure 1). Group  $G_1$  is mainly dominated by three taxa within the order  
 212 *Clostridiales* (family *Ruminococcaceae* (2) and gender *Blautia*) and one taxon within  
 213 the gender *Actinomyces*. Two taxa (*g\_Veillonella* and *f\_Lachnospiraceae*) have a  
 214 coefficient close to zero and will have a very small contribution to the signature. Group  
 215  $G_2$  is composed by two taxa within the genders *Haemophilus* and *Staphylococcus*. Note  
 216 that the selected taxa within the microbial signature are among most important taxa  
 217 according to the results of the pairwise log-ratio analysis (Table 1).

218

219 Table 2. Taxa included in the microbiome signature that best discriminates between the two diet  
 220 groups

Balance group	Coefficient	Taxonomic assignment
$G_1$	0.3359	<i>p_Firmicutes;c_Clostridia;o_Clostridiales;f_Ruminococcaceae;g_1</i>
	0.2730	<i>p_Firmicutes;c_Clostridia;o_Clostridiales;f_Lachnospiraceae;g_Blautia</i>
	0.2159	<i>p_Actinobacteria;c_Actinobacteria;o_Actinomycetales;f_Actinomycetaceae;g_Actinomyces</i>
	0.1358	<i>p_Firmicutes;c_Clostridia;o_Clostridiales;f_Ruminococcaceae;g_2</i>
	0.0337	<i>p_Firmicutes;c_Clostridia;o_Clostridiales;f_Veillonellaceae;g_Veillonella</i>
	0.0055	<i>p_Firmicutes;c_Clostridia;o_Clostridiales;f_Lachnospiraceae;g_</i>
$G_2$	-0.4327	<i>p_Proteobacteria;c_Gammaproteobacteria;o_Pasteurellales;f_Pasteurellaceae;g_Haemophilus</i>
	-0.5672	<i>p_Firmicutes;c_Bacilli;o_Bacillales;f_Staphylococcaceae;g_Staphylococcus</i>

221

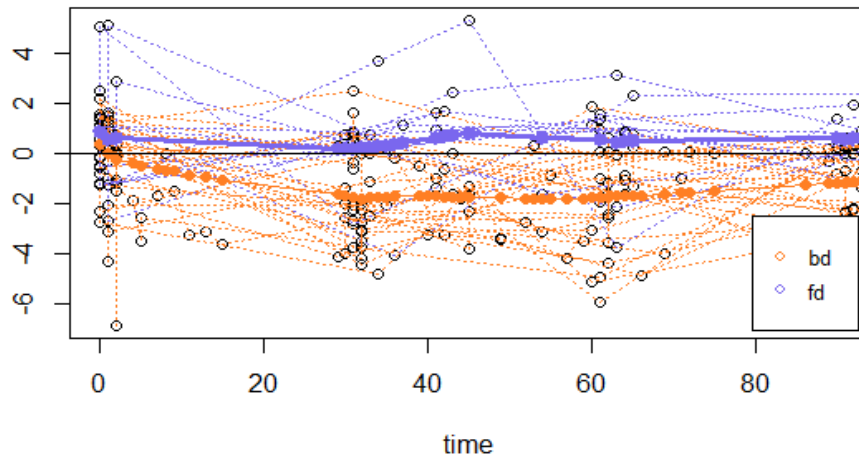


222

223 Fig 1. Taxa composing the microbiome signature that best discriminates between the two diet  
224 groups (green: positive coefficient and red: negative coefficient)

225

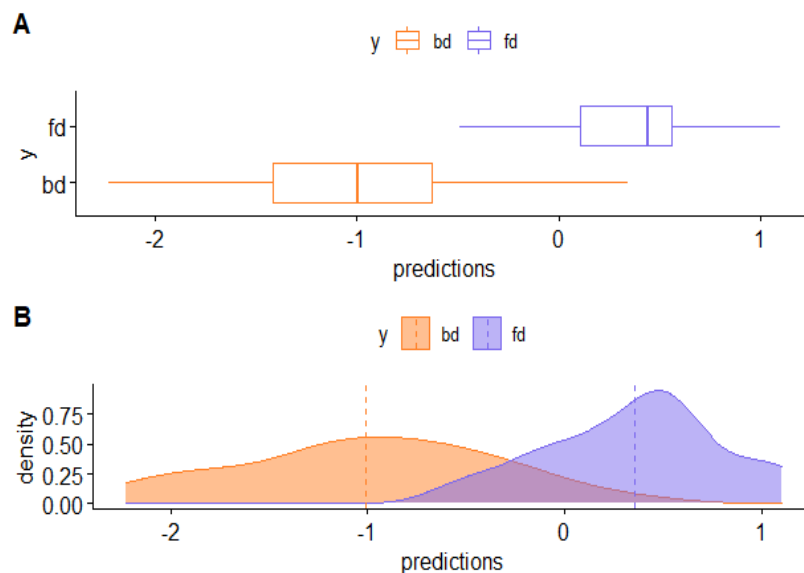
226 The trajectories of the microbial signature over the observed period are represented in  
227 Figure 2, where the color of the curves corresponds to the diet group. Each trajectory  
228 represents the relative mean abundances between the two taxa groups for each child. We  
229 can see that the two groups are clearly separated. Those children under breastmilk diet  
230 (in orange) usually have trajectories below zero, which means they have more relative  
231 mean abundance of *g\_Haemophilus* and *g\_Staphylococcus* with respect to the relative  
232 abundance of taxa in group  $G_1$ , while children with formula milk diet (in blue) have  
233 more relative abundance of taxa in group  $G_1$  relative to  $G_2$ .



234

235 Fig 2. Relative abundance between group  $G_1$  and  $G_2$  during the first three months of life.  
236 Highlighted curves represent the mean value of the signature for each diet group  
237 (orange: breast milk diet, blue: formula milk diet)  
238

239 Figure 3 displays the distribution of the microbial signature scores for the two diet  
240 groups and offers a visual assessment of the (apparent) discrimination accuracy of the  
241 signature. Quantitatively, the apparent discrimination accuracy of the signature (i. e. the  
242 AUC of the signature applied to the same data that was used to generate the model) is  
243 0.96 and the mean cross-validation AUC is 0.74 (sd=0.10).  
244



245

246 Fig 3. Distribution of the microbial signature scores for the two diet groups  
247 (orange: breast milk diet, blue: formula milk diet)  
248  
249

250 Both results, the pairwise analysis and the taxa selected in the microbial signature, are  
251 consistent with previous studies on the association of the infant gut microbiome  
252 composition and breastmilk feeding practices. In Fehr et al. (2020), *Haemophilus*  
253 *parainfluenzae* and *Staphylococcus* were found to be enriched with exclusive breastmilk  
254 feeding together with lower prevalence of *Actinomyces* at 3 months. *Lachnospiraceae*  
255 (*Blautia*) was enriched among infants who were no longer fed breastmilk. Similar  
256 results are reported in Laursen et al. (2016) where the duration of exclusive  
257 breastfeeding was negatively correlated with genera within *Lachnospiraceae* (e.g.,  
258 *Blautia*) and genera within *Ruminococcaceae*. Positive correlations with exclusive  
259 breastfeeding were observed for *Bifidobacterium* and *Pasteurellaceae*  
260 (*Haemophilus*).

#### 261 **4. Discussion**

262 Longitudinal microbiome studies, especially those focused on the human microbiome,  
263 have usually low resolution: the number of individuals is small, each individual has few  
264 observation times, the observations of the different individuals are not made at exactly  
265 the same time, the data are very variable, the expected behavior of the abundance  
266 trajectories is not linear or quadratic, etc. This makes it difficult to justify and  
267 implement a parametric modeling of trajectories and limits the use of models for  
268 longitudinal data (time series, mixed models). In this context, a description of the  
269 trajectories such as the one we propose, although less precise, allows to extract valuable  
270 information from the data as we have shown in the example. Other longitudinal data  
271 modeling strategies (Gerberg et al. 2012, Park et al. 2020, Silverman et al. 2018, Äijö et  
272 al. 2017) could be used in longitudinal microbiome studies with higher resolution such  
273 as laboratory or animal experimental studies.

274 The applicability of CoDA methods in microbiome studies has been limited by the  
275 difficulty in interpreting the obtained results. We hope that this work and the R package  
276 “coda4microbiome” will help to increase the use of these methods in this field.

## 277 **Acknowledgements**

278 This work was partially supported by the Spanish Ministry of Economy, Industry and  
279 Competitiveness, Reference PID2019-104830RB-I00.

## 280 **Data Accessibility**

281 The filtered data from the ECAM study is available as a data object in the  
282 “coda4microbiome” package.

## 283 **References**

- 284 1. Äijö T, Müller CL and Bonneau R. Temporal probabilistic modeling of bacterial  
285 compositions derived from 16S rRNA sequencing. *Bioinformatics*, 34(3), 2018,  
286 372–380 doi: 10.1093/bioinformatics/btx549
- 287 2. Aitchison J. *The Statistical Analysis of Compositional Data*. London: Chapman &  
288 Hall, 1986.
- 289 3. Aitchison J. and Bacon-Shone J. Log contrast models for experiments with  
290 mixtures. *Biometrika*. 1984, 71: 323–330.
- 291 4. Bokulich NA, Chung J, Battaglia T, Henderson N, Jay M, Li H, Lieber AD, Wu F,  
292 Perez-Perez GI, Chen Y, Schweizer W, Zheng X, Contreras M, Dominguez-Bello  
293 MG, Blaser MJ. Antibiotics, birth mode, and diet shape microbiome maturation  
294 during early life. *Sci Transl Med*. 2016, 8:343ra82.  
295 <https://doi.org/10.1126/scitranslmed.aad7121>
- 296 5. Bokulich NA, Dillon MR, Zhang Y, Rideout JR, Bolyen E, Li H, Albert PS,  
297 Caporaso JG. q2-longitudinal: longitudinal and paired-sample analyses of

- 298 microbiome data. *mSystems*. 2018, 3:e00219-18.  
299 <https://doi.org/10.1128/mSystems.00219-18>. Microbiome Data
- 300 6. Calle ML. Statistical analysis of metagenomics data. *Genomics Inform*. 2019, 17(1):  
301 e6
- 302 7. Calle ML, Susin A, coda4microbiome R-package (CRAN). 2022
- 303 8. Fehr K, Moossavi S, Sbihi H, Finlay B, Turvey SE, Azad MB. Breastmilk Feeding  
304 Practices Are Associated with the Co-Occurrence of Bacteria in Mothers' Milk and  
305 the Infant Gut: the CHILD Cohort Study. *Cell Host & Microbiome*. 2020,  
306 28(2):285-297.e4 <https://doi.org/10.1016/j.chom.2020.06.009>
- 307 9. Gerber GK, Onderdonk AB, Bry L. Inferring Dynamic Signatures of Microbes in  
308 Complex Host Ecosystems. *PLoS Comput Biol*. 2012, 8(8): e1002624.  
309 <https://doi.org/10.1371/journal.pcbi.1002624>
- 310 10. Gloor, Gregory B and Wu, Jia Rong and Pawlowsky-Glahn, Vera and Egozcue,  
311 Juan José It's all relative: analyzing microbiome data as compositions. *Annals*.  
312 *Epidemiology*. 2016, 26(5):322-9.  
313 <http://dx.doi.org/10.1016/j.annepidem.2016.03.003>
- 314 11. Gloor GB. and Reid G. Compositional analysis: a valid approach to analyze  
315 microbiome high throughput sequencing data. *Can J Microbiol*. 2016, 62(8):692–  
316 703. <http://dx.doi.org/10.1139/cjm-2015-0821>
- 317 12. Laursen MF, Andersen LBB, Michaelsen KF, Mølgaard C, Trolle E, Bahl MI, Licht  
318 TR. Infant gut microbiota development is driven by transition to family foods  
319 independent of maternal obesity. *MSphere*. 2016, 1(1): e00069-15.  
320 [doi:10.1128/mSphere.00069-1](https://doi.org/10.1128/mSphere.00069-1)



- 321 13. Park Y, Ufodu A, Lee K, Jayaraman A, Emerging computational tools and models  
322 for studying gut microbiota composition and function, Current Opinion in  
323 Biotechnology. 2020, 66: 301-311. <https://doi.org/10.1016/j.copbio.2020.10.005>.
- 324 14. Schmidt T, Raes J., Bork P. The Human Gut Microbiome: From Association to  
325 Modulation, Cell. 2018, 172: 1198-1215. <https://doi.org/10.1016/j.cell.2018.02.044>
- 326 15. Silverman JD, Durand HK, Bloom RJ, Mukherjee S, David LA. Dynamic linear  
327 models guide design and analysis of microbiota studies within artificial human guts.  
328 Microbiome. 2018, 6:202. <https://doi.org/10.1186/s40168-018-0584-3>
- 329 16. Susin A, Wang Y, Lê Cao KA, Calle ML. Variable selection in microbiome  
330 compositional data analysis. NAR Genomics and Bioinformatics. 2020, 2 (2):  
331 lqaa029, <https://doi.org/10.1093/nargab/lqaa029>